Annals of Biomedical Engineering, Vol. 26, pp. 502–511, 1998
Printed in the USA.

0090-6964/98 $10.50 + .00

A Novel Method for Efficient Drug Delivery

CHRISTOS P. MARKOU,* ELIZABETH M. LUTOSTANSKY,† DAVID N. KU,† and STEPHEN R. HANSON*

*Department of Medicine, School of Medicine, Division of Hematology/Oncology, Emory University, Atlanta, GA and
†G. W. Woodruff School of Mechanical Engineering, Georgia Institute of Technology, Atlanta, GA

(Received 13 February 1997; accepted 29 October 1997)

Abstract—Local delivery of anti-thrombotic and anti-restenotic drugs is desired to achieve high concentrations of agents which may be rapidly degraded systemically or which exhibit very short half-lives *in vivo*. In this article, the operating characteristics of a novel local drug delivery method are described and its effectiveness demonstrated computationally and experimentally. Computational models used a finite volume method to determine the concentration field. Optical dye density measurements of Evans blue in saline were performed in an *in vitro* steady flow system. Modeling parameters were kept in the physiologic range. Experimental flow visualization studies demonstrated high concentrations of infusate near the vessel wall. Computational studies predicted high, clinically significant drug concentrations along the wall downstream of the infusion device. When the radial infusion velocity is large (infusion flow rate, $Q_{inf} > 0.5\%$ of the main flow rate, Q), the wall concentration of the infused drug remains high, e.g., levels are greater than 80% of the infusate concentration 5 cm downstream of the infusion device. At lower infusion rates ($Q_{inf} < 0.001Q$), the drug concentration at the wall decreases exponentially with axial distance to less than 25% of the infusate concentration 5 cm downstream of the infusion device, although therapeutic drug levels are still readily maintained. The near wall drug concentration is a function of flow conditions, infusion rate, and the drug diffusivity. Good agreement was obtained between computational and experimental concentration measurements. Flow simulation and experimental results indicate that the technique can effectively sustain high local drug concentrations for inhibition of thrombosis and vascular lesion formation. © *1998 Biomedical Engineering Society.*
[S0090-6964(98)01403-9]

Keywords—Local drug delivery, Mass transfer, Blood-materials interactions.

INTRODUCTION

Thrombosis and arteriosclerosis are clinically important in the development of acute cardiovascular episodes such as myocardial infarction, angina, stroke, and obstructive peripheral vascular disease. Repeated thrombotic events promote the development of atherosclerotic vascular lesions. In addition, thrombus formation often complicates interventional cardiovascular procedures for revascularization of obstructed arteries (e.g., angioplasty).

Current methods of controlling thrombo-occlusive events include the systemic administration of anticoagulant agents such as heparin. Systemic delivery of antithrombotic and antirestenotic drugs is expensive and may cause serious side effects such as bleeding. It is difficult to provide controlled therapy over long time periods. There may be systemic intolerance at the high doses required for effective therapy. The cost of production in combination with the drug quantity needed may be prohibitive for use. Finally, administration of the drugs may require hospitalization, which is associated with the increased cost of health care.

Local drug delivery is advantageous because it is possible to achieve very high local concentrations of agents at the exact vascular wall sites where treatment is needed. These drugs provided systemically could otherwise be rapidly degraded or removed. Localized drug delivery reduces the side effects of systemic delivery, such as the risk of hemorrhage. Other advantages of local delivery include: (1) agents which may be administered over extended time periods, (2) very small quantities of toxic drugs delivered locally which may produce no systemic effects and therefore may be sustainable by the human body, and (3) the overall cost of treatment, which will be significantly lowered by reducing the amount of drugs and the administration costs.

Two discrete approaches can effect local treatment: (a) biochemical targeting—consisting of systemically delivered drugs that act locally, and (b) anatomic targeting—methods delivering high drug concentrations at specific sites.[20] Previously described local delivery anatomic targeting methods have employed various types of devices.[12,18] One type of local delivery device involves drug-loaded polymers that either coat surfaces (e.g., stents) or are implanted directly. These drug-containing polymer-based systems release therapeutic agents as the polymer slowly dissolves or degrades. Other types consist of balloon catheter delivery systems

Address correspondence to Stephen R. Hanson, Ph.D., 1639 Pierce Drive, Room 1129, Division of Hematology/Oncology, Department of Medicine, School of Medicine, Emory University, Atlanta, GA 30322.

which locally deliver pharmacologic agents through a porous balloon which is threaded into the target blood vessel. Local drug delivery can also be achieved by a straight type catheter with side holes and through facilitated diffusion of a drug through the arterial wall (e.g., iontophoresis).

As an alternative to these devices, a new local delivery approach was developed. The device delivers high levels of active agents to specific sites while minimizing the disruption of blood flow. The principle of operation of the device is infusion of anti-thrombotic and other drugs through a porous membrane in line with the vessel wall. Because of the large surface area of the membrane and the low infusion rates, the radial velocity of the drug into the blood flow is very low compared to the main flow. Therefore, the disruption of normal axial blood flow caused by the drug infusion is limited. The infused agents are transported downstream and remain adjacent to the wall by convection forces. Radial diffusion of the agents is slow compared to axial convection. The most obvious application of this approach is for the prevention of thrombosis and intimal hyperplasia at the distal end of synthetic vascular grafts. The usefulness and limitations of this local drug delivery approach for grafts and other applications are discussed subsequently.

The local drug delivery approach takes advantage of the low flow velocities in the near wall region. Thus, for steady tube flow, the outer annular ring which contains 10% of the tube's cross sectional area near the wall transports only about 1% of the total volume flow.[1] Drug infusion in this near wall region allows higher concentrations to be maintained adjacent to the vessel wall. Another advantage of this delivery approach is that therapeutic agents can be delivered over long time periods, rather than the short time periods permitted by balloon delivery catheters. The efficacy of the present local drug delivery device has been demonstrated in preliminary animal experiments.[3,22] This article provides the theoretical basis for this novel local drug delivery method, quantifies the drug concentration levels achievable downstream of the device, and describes the operating range of local infusion rates. Finally, these results can be used to estimate drug concentration levels in other studies involving local intravascular drug delivery.

METHODS

Computational and experimental methods were employed to characterize local drug delivery. The computational method allowed simulation of infusion of different agents into blood flow at various rates and calculation of agent concentrations in the flowfield. The experimental method provided a qualitative and visual means to assess local infusion characteristics and verification of the computational results.

TABLE 1. Diffusivity and Schmidt number of several molecules of interest. Values determined by Stokes drag as described in text.

Molecule	Diffusivity	Schmidt number
NO	10^{-9} m^2/s (in blood)	1170
Heparin	10^{-10} m^2/s (in blood)	11,700
Thrombin	4×10^{-11} m^2/s (in blood)	29,300
Evans blue	3×10^{-10} m^2/s (in saline)	3300

Numerical Approach

The mass transfer downstream of the drug delivery site was modeled computationally to quantify the concentration of the infused drug near the wall. The quantification of the drug concentration is necessary to ensure that the concentration at the wall is high enough for successful therapy. To illustrate the usefulness of computational methods for modeling a local infusion device, the near wall concentration of drug infused at the wall of a straight axisymmetric tube was determined and compared with experimental results.

Model Description. The blood conduit tube and local delivery device tube had a diameter of 4 mm, consistent with the size of medium diameter arteries. At the wall, a drug was infused through a 1 cm slit around the circumference of the tube to model the infusion area of the delivery device. The drug was infused in a purely radial direction at a constant and uniform velocity. It was assumed that the delivery of the drug through the slit was uniform. The wall boundary downstream of the infusion location was assumed to be an inert material with zero mass flux through the wall. The wall boundary condition was identical to the boundary conditions in the *in vitro* experimental models using glass tubes, described in the following section. A zero mass flux at the wall is physiologically relevant when the permeability of the arterial wall to the drug is extremely low and the event is reaction limited. The drug concentration at the wall downstream of the infusion device was determined for several different agents and infusion rates.

The diffusivities of the agents infused, heparin, thrombin and nitric oxide (NO), in blood were approximated using Stokes' drag. The diffusivity values used in the numerical models are given in Table 1. The diffusivity of Evans blue dye in saline was approximated by the same formula. This relationship uses the particle size to determine diffusivity,

$$D=\frac{\kappa T}{6\pi\mu R},$$

where D is the diffusion coefficient, κ is the Boltzmann constant (1.38×10^{-23} J/K/molecule), T is assumed to be

the body temperature (310 K), μ is the fluid dynamic viscosity, and R is the particle radius. This analysis assumes that the particles are spherical and in a dilute suspension. The diffusion coefficients employed were selected in order to differ by an order of magnitude. Earlier studies for NO and heparin showed that the estimated diffusion coefficients used were in good agreement with experimentally measured values (see Refs. 8 and 13, respectively). The Reynolds number ($\mathrm{Re}=Ud/\nu$; U is the mean flow velocity, d is the vessel diameter, and ν is the kinematic viscosity of the fluid) relates inertia and viscous forces. In all computer models and subsequent experiments the Reynolds number was kept constant ($\mathrm{Re}=140$). This simulates blood flow of 100 ml/min in a 4 mm artery. The Schmidt number is a dimensionless parameter which relates convective and diffusive mass transfer. The Schmidt number is defined as $\mathrm{Sc}=\nu/D$, where ν is the kinematic viscosity of the fluid and D is the particle diffusivity.

Boundary Conditions. At the inlet, the flow was assumed to be steady and fully developed. The drug concentration at the inlet was zero. At the walls, a no-slip boundary condition was used. In addition, the walls were assumed to be inert with no mass flux normal to the wall. The outlet boundary conditions were such that the streamwise gradients of the velocity field and the concentration field are small. The validity of this boundary condition was insured by extending the outlet sufficiently far downstream so that further extension had negligible effect on the flow field. At the infusion location, the drugs were infused in a purely radial direction at a uniform velocity. The infusion rate, Q_{inf}, was varied between 0.01 ml/min and 1 ml/min.

Numerical Methods. To model the effects of the local drug infusion on the concentration and velocity field downstream of the infusion location, a computational code, FLUENT (Fluent Inc., Lebanon, NH), was used. To numerically solve the governing equations, the domain was discretized into finite control volumes using an axisymmetric Cartesian grid. In all cases, fine grid spacing was needed near the wall due to the thin concentration boundary layer that occurs with low particle diffusivity. In addition, fine grid spacing was needed in the infusion region because of the large velocity and concentration gradients in this area. A grid with 230 nodes in the axial direction and 52 nodes in the radial direction was used. The closest grid point to the tube wall was located at 99.9% of the tube radius.

The governing differential equations are approximated by a set of algebraic equations which must be evaluated at each node. The solutions to the algebraic equations produced a set of discrete values which are approximate solutions to the governing partial differential equations. The FLUENT code uses the SIMPLE algorithm. This is a semi-implicit iterative scheme. A quadratic upwinding scheme is used to interpolate between grid points and to calculate the derivatives of the flow variables.

The grid independence was verified by comparing the wall concentration and wall shear stress in the original grid with the values in a doubled grid (double density). The variation in wall concentration and wall shear stress between the two grids was less than 3% for all cases. In order to validate the computational results, the results of the computational model of dye infusion were compared with experimental results.

Experimental Approach

Dye visualization and concentration measurement techniques were used to experimentally determine the concentration levels achievable by the local infusion device. Local infusion of Evans blue dye was performed using a device that delivers the infusate circumferentially. The device was constructed from a 1.0 cm microporous and ringed expanded polytetrafluoroethylene (ePTFE, 4.0 mm i.d) clinical graft material (Gore-Tex, W.L. Gore and Associates, Inc). A cuff reservoir from 5.0 mm i.d. silicone rubber tubing (Silastic, Dow Corning) was placed over the ePTFE graft. Evans blue dye was infused into the reservoir space between the graft and the cuff through a length of 0.64 mm i.d. Silastic tubing was inserted through the wall of the 5.0 mm i.d. cuff. As described earlier, the infusate filled the reservoir space, passed through the wall of the porous ePTFE graft, and entered the slow moving fluid layers at the interface between the fluid and the wall.[22]

The flow system was driven by a Masterflex pump which provided a steady flow of saline at a flow rate of 27 ml/min to simulate the blood flow used in the experiments. Flow development was achieved by the inclusion of a long entrance tube upstream of the infusion device. The entrance and downstream tubes were 4 mm i.d. glass tubes connected to the infusion device with silicon rubber glue (Silastic Medical Adhesive, Dow Corning). The Evans blue dye was infused through the local delivery device shown in Figure 1. The infusion rate was varied between 0.01 and 1 ml/min by the syringe pump (Harvard Apparatus, Natick, MA). Downstream of the infusion device, the drug concentration near the wall was measured using fluid withdrawal.

The method of near-wall sample withdrawal—called hole sampling—used hypodermic tubing (i.d.$=0.25$ mm) attached to a syringe pump. The hypodermic tubing was positioned in a small hole drilled into the glass tube 3 cm from the end of the infusion site. Dye samples were withdrawn through the hypodermic tubing at an extremely low rate (0.005 ml/min) to minimize the influence of the withdrawal on the blood flow, according to

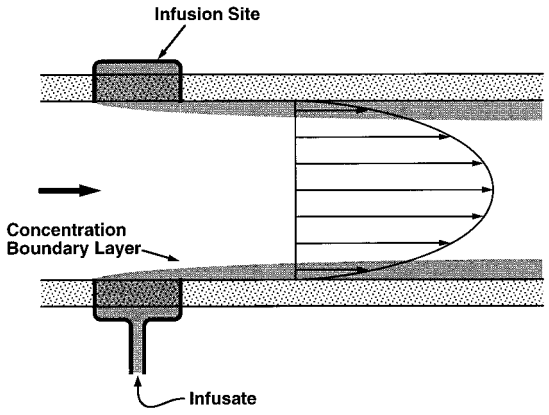

FIGURE 1. Qualitative schematic of the local infusion principle (not to scale).

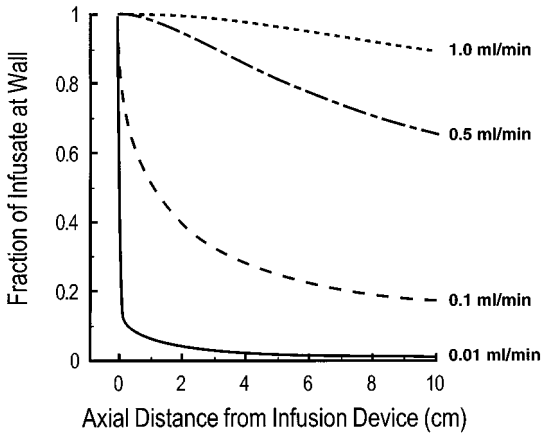

FIGURE 2. Normalized concentration of infused Evans blue dye at the wall downstream of the infusion site for four different infusion rates (main flow rate of saline=27 ml/min, Sc=3300, Re=140).

previously published studies that suggest the range of withdrawal parameters with respect to main flow conditions, in order to avoid disturbances in the flowfield.[19]

The concentration of the fluid samples was quantified using a spectrophotometer (Gilford Response, Ciba Corning, Medfield, MA), which measured light transmission through a 1 ml fluid sample at a wavelength of 595 nm. Dye concentrations at specific sites downstream of the infusion device could be directly compared to the numerical results.

RESULTS

Numerical Results

For the specific agents studied, there were two regimes of drug infusion rate. At high infusion rates on the order of 1 ml/min, the infused drug concentration was maintained at high levels on the wall over relatively long distances downstream from the infusion site. At lower infusion rates, the concentration of the drug adjacent to the wall decreased exponentially with axial distance.

The drug concentration at the wall is a function of infusion rate as illustrated in Figure 2. The normalized concentration is given as the fraction of infusate concentration, $x_i = C_i / C_{\text{initial}}$. The wall concentration of Evans blue downstream of the infusion device is shown for infusion rates of 0.01, 0.1, 0.5 and 1.0 ml/min. The main flow rate of saline, Q, was 27 ml/min. For the lower infusion rates, 0.01 and 0.1 ml/min, the concentration of Evans blue at the wall decreased to less than 20% of the inlet concentration within 10 cm of the infusion device. At higher infusion rates of 0.5 and 1.0 ml/min, the Evans blue concentration at the wall remained above 60% of the inlet concentration for the first 10 cm downstream from the infusion device. The large difference in the Evans blue concentration at the wall for the lower (0.01 and 0.1 ml/min) and higher (0.5 and 1.0 ml/min) infusion rates is also evident from the thickness of the concentration boundary layer.

Figure 3 shows the thickness of the Evans blue concentration boundary layer (99% level) as a function of the axial distance downstream from the infusion device for a main flow rate of 27 ml/min. The thickness of the concentration boundary layer, δ_c, is normalized with the tube radius, R, and depends strongly on the infusion rate. The concentration boundary layer thickness increases with increasing infusion rate and with axial distance. For infusion rates of 0.5 and 1.0 ml/min, the concentration boundary layer extends to more than 10% of the tube radius. For possible clinical applications and in order to reduce the amount of drug infused, it is desirable to keep the infused drug in a thin concentration boundary layer, e.g., less than 10% of the tube radius.

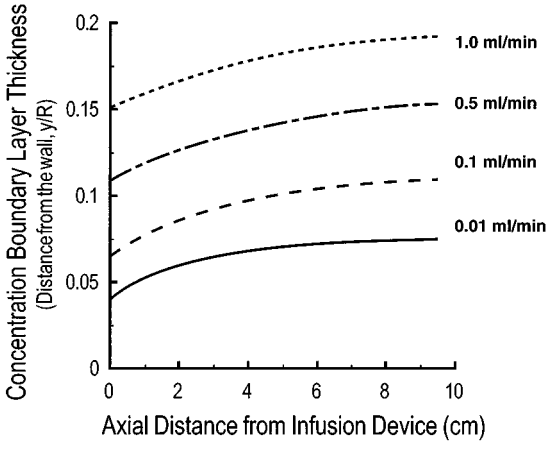

FIGURE 3. Evans blue concentration boundary layer thickness growth for four different infusion rates (main flow rate of saline=27 ml/min, Sc=3300, Re=140).

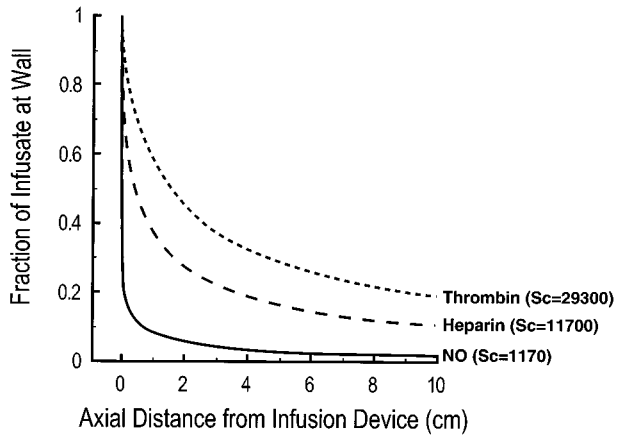

FIGURE 4. Concentration of three infused substances at the wall. NO exhibits a lower concentration at the wall due to its enhanced diffusivity (main flow rate=100 ml/min, infusion rate=0.05 ml/min, Re=400).

The drug concentration downstream of the infusion device is also a function of the diffusivity of the infused agent, as shown in Figure 4. The infusate concentrations at the wall for NO, heparin, and thrombin are illustrated for an infusion rate of 0.05 ml/min and a main blood flow rate of 100 ml/min. Thrombin has the lowest diffusivity; therefore, its concentration gradients are expected to be the sharpest. The sharp concentration gradient and corresponding thin concentration boundary layer result in a higher thrombin concentration at the wall than heparin or NO concentrations under identical conditions.

The molecular diffusivity also affects the thickness of the concentration boundary layer as shown in Figure 5. Under the same flow conditions as for Figure 4, the thickness of the concentration boundary layer for thrombin is less than 4% of the tube radius at 10 cm downstream of the infusion device. For smaller, more diffusive molecules such as heparin and NO, the concentration boundary layer is thicker and the drug concentration at the wall is lower.

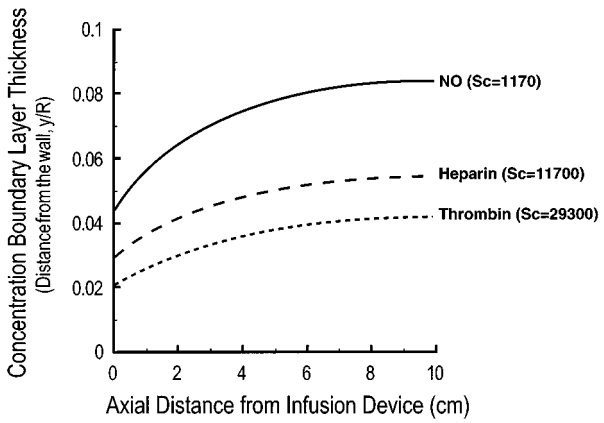

FIGURE 5. Drug concentration boundary layer thickness downstream of the infusion site. The boundary layer thickness of NO increases rapidly because of its high diffusivity away from the wall (main flow rate=100 ml/min, infusion rate=0.05 ml/min, Re=400).

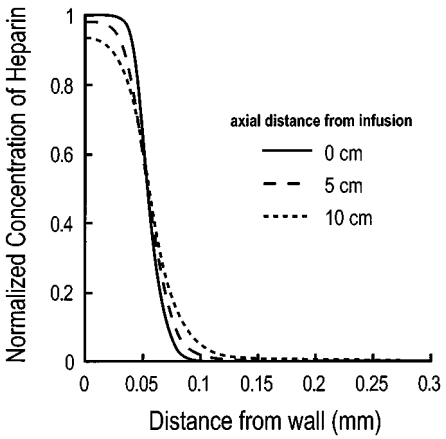

FIGURE 6. Near wall concentration profiles for heparin in blood at three sites downstream of infusion site (main flow rate=100 ml/min, infusion rate=1 ml/min).

The concentration profiles in the radial direction downstream of the infusion location illustrate the different mass transfer phenomena at high and low infusion rates. At high infusion rates, the infused drug penetrates into the main flow field. At lower infusion rates, the infused drug remains in the near wall region as intended. In Figure 6, the normalized concentration of heparin is shown as a function of the distance from the wall at the infusion site $(x=0)$ and at 5 and 10 cm downstream from the infusion site for an infusion rate of 1 ml/min. The main flow rate was 100 ml/min. At the infusion site, the essentially pure drug extends radially into the flow field. The wall concentration of heparin remains above 90% of the infused concentration 10 cm downstream of the infusion location.

At a lower heparin infusion rate of 0.1 ml/min, the near wall drug concentration at the infusion location is approximately 90% of the drug infusion concentration, as shown in Figure 7. The near-wall drug concentration rapidly decreases to 20% of the inlet concentration 10 cm downstream of the infusion location. The concentration boundary layer for an infusion rate of 0.1 ml/min is much thinner than for an infusion rate of 1 ml/min.

The CFD solutions illustrate the influence of particle diffusivity and infusion rate on the concentration field downstream of the infusion device. The concentration field is also expected to be influenced by the main flow rate. To demonstrate the validity of the CFD results, dye visualization experiments were performed.

Experimental Results

Experimental models included dye visualization studies to illustrate that drugs infused by the local delivery

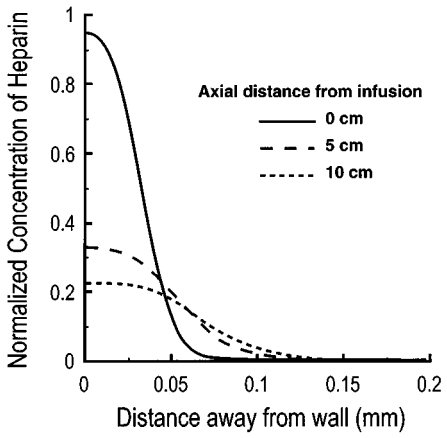

FIGURE 7. Near-wall concentration profiles for heparin in blood at three sites downstream of infusion site (main flow rate=100 ml/min, infusion rate=0.1 ml/min).

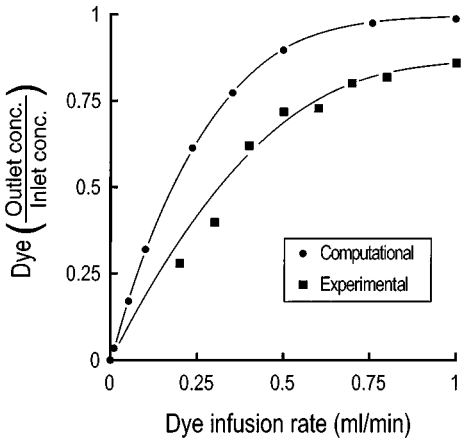

FIGURE 9. Evans blue concentration at the wall measured 3 cm downstream of infusion device as a function of infusion rate. Comparison of computational and experimental measurements.

device would remain in the near-wall region. Figure 8 illustrates a cross sectional view of the drug delivery device. The left side of the figure shows the device with only saline infused. The white ring is the ePTFE material. Outside of the ePTFE graft is a narrow annular ring which is the space in the cuff reservoir (large arrow). The right side of the figure illustrates the infusion of Evans blue dye in saline. The dye is pumped by the syringe pump through the silastic tubing shown at the bottom of the figure. The dye fills the chamber around the ePTFE graft. The dye which passes through the graft remains in the near-wall region, as identified by the three small arrows.

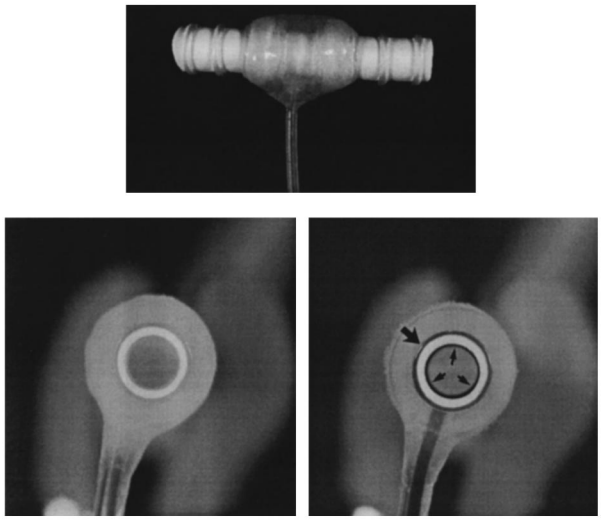

FIGURE 8. Flow visualization of cross section of infusion device–infusion of saline (left), infusion of Evans blue into main flow of saline (right). The top presents a side view of the ePTFE graft local infusion device.

In addition to visually confirming the near-wall drug delivery through dye visualization studies, the dye concentration near the wall was determined experimentally. Quantification of the dye concentration was desired to show that numerical methods could accurately predict concentration levels of dyes and anti-thrombotic drugs.

The Evans blue dye concentrations of fluid samples withdrawn 3 cm downstream of the infusion device were measured by the hole sampling technique. The measured concentrations were compared with the numerical calculations. Concentration values were compared for several infusion rates between 0.01 and 1 ml/min. The main flow rate of saline was 27 ml/min. A comparison is shown in Figure 9. The concentration levels at the wall increased with increasing infusion rates as expected based on the results shown in Figure 2. The numerically predicted concentration values were always greater than the experimentally measured values for all infusion rates. The concentration levels measured by the hole sampling were lower than the predicted levels, suggesting the sampling of fluid layers further away from the wall in hole sampling. That this is indeed the explanation is suggested by the observations in Figure 9 that the discrepancy between the numerical and experimental wall dye concentrations is greatest at the lowest infusion rates which would produce thinner boundary layers (and hence the greatest wall sample dilution by deeper fluid layers under conditions of fixed sample withdrawal rate).

For infusion rates greater than 0.5 ml/min, the experimental and numerical results illustrate that under the specified flow conditions (Evans blue dye in saline, $Q=27$ ml/min, 4 mm impermeable tubing), the concentration of the dye at the wall remains above 50% of the infused concentration 3 cm downstream of the infusion device. Based on the good agreement between the nu-

merical and experimental models of the infusion device, the local delivery device is an efficient means of achieving high local concentrations while reducing total drug volume requirements.

Scaling Analysis

Scaling analysis can assist in the interpretation and correlation of experimental data by reducing the number of variables necessary to define a solution. Scaling analysis is empirical and can also provide the appropriate relationship between variables to obtain similar solutions. Figure 2 shows a distinct difference in the wall concentration as a function of the drug infusion rate. For the therapeutically significant infusion rates of 0.5 ml/min and lower, an exponential decline of drug wall concentration was observed.

The continuity equation for tube flow in cylindrical coordinates is

$$\frac{\partial \rho}{\partial t}+\frac{1}{r}\frac{\partial}{\partial r}(\rho r V_r)+\frac{1}{r}\left(\frac{\partial}{\partial \theta}(\rho V_\theta)\right)+\frac{\partial}{\partial z}(\rho V_z)=0 \quad (1)$$

where ρ is the density, V_r is the radial velocity, V_θ angular velocity, and V_z is the axial velocity. In the case of steady, axisymmetric flow the first and third terms are zero. Dividing by ρ the equation simplifies to

$$\frac{\partial V_r}{\partial r}+\frac{V_r}{r}+\frac{\partial V_z}{\partial z}=0. \quad (2)$$

Scaling the terms of the above equation in the hydrodynamic boundary layer:

$$\frac{V_r}{\delta}, \frac{V_r}{\delta}, \frac{U}{L},$$

where the tube diameter, D, is the length scale in the radial direction, the flow velocity, U, is the velocity scale in the axial direction, and the tube length, L, is the length scale in the axial direction. All the terms must be of the same order of magnitude, resulting in

$$V_r \approx \frac{U\delta}{L}. \quad (3)$$

For the concentration boundary layer, the terms of the continuity equation (2) can be scaled with δ_c as the length scale:

$$\frac{V_r}{\delta_c}, \frac{V_r}{\delta_c}, \frac{U(\delta_c/D)}{L}.$$

From the above:

$$V_r \approx \frac{U\delta_c^2}{DL}. \quad (4)$$

The species conservation equation is

$$\frac{\partial C}{\partial t}+V_r\frac{\partial C}{\partial r}+\frac{V_\theta}{r}\frac{\partial C}{\partial \theta}+V_z\frac{\partial C}{\partial z} = \frac{r^m}{\rho}+D_{12}\left[\frac{1}{r}\frac{\partial}{\partial r}\left(r\frac{\partial C}{\partial r}\right)+\frac{1}{r^2}\frac{\partial^2 C}{\partial \theta^2}+\frac{\partial^2 C}{\partial z^2}\right], \quad (5)$$

where C is the species concentration and D_{12} the diffusivity. The first term on the right hand side can be neglected (no species generation), as well as the unsteady term and the terms related to angular symmetry. Equation (5) can be written as

$$V_r\frac{\partial C}{\partial r}+V_z\frac{\partial C}{\partial z}=D_{12}\left(\frac{\partial^2 C}{\partial r^2}+\frac{1}{r}\frac{\partial C}{\partial r}+\frac{\partial^2 C}{\partial z^2}\right). \quad (6)$$

Scaling (6) and using (4) the terms of the above equation can be presented as

$$\frac{U\delta_c^2}{DL}\frac{\Delta C}{\delta_c}, \; U\frac{\delta_c}{D}\frac{\Delta C}{L}, \; D_{12}\frac{\Delta C}{\delta_c^2}, \; D_{12}\frac{1}{\delta_c}\frac{\Delta C}{\delta_c}, \; D_{12}\frac{\Delta C}{L^2}.$$

If $L \gg \delta_c$ (i.e., the boundary layer is small), then the last term is very small compared to the others. Therefore,

$$\frac{U\delta_c}{D}\frac{\Delta C}{L} \approx D_{12}\frac{\Delta C}{\delta_c^2} \quad \text{and} \quad \delta_c^3 \approx \frac{D_{12}DL}{U}$$

or

$$\delta_c \approx \left(\frac{D_{12}DL}{U}\right)^{1/3}. \quad (7)$$

Substituting (7) into (4) and using the Reynolds (Re) and Schmidt (Sc) numbers we get

$$V_r \approx U\ \mathrm{Sc}^{-2/3}\mathrm{Re}^{-1}, \quad (8)$$

which provides a relationship between the infusion velocity and the main flow. Using the aforementioned expression, the limiting infusion velocity can be determined from the Reynolds number, the Schmidt number, and the axial fluid velocity. The infusion rates are calculated from the radial velocity and the area of the infusion slit. Below the critical infusion rate, the boundary layer ap-

proximation is valid and the wall concentration of the drug decreases exponentially with axial location. Above the limiting infusion rate, the boundary layer analysis is not valid due to the large radial velocity at the site of infusion. Due to the high infusion rate, the drug penetrates into the main flow. By keeping the infusion rate below the limiting infusion rate, the infused drug remains in the near-wall region where it is needed.

The limiting infusion velocity, V_r, can also be expressed in terms of the ratio of the infusion rate and the main flow rate as shown below:

$$\frac{Q_{\text{infu}}}{Q_{main}} \approx \frac{4l}{D} \text{Sc}^{-2/3} \text{Re}^{-1}, \tag{9}$$

where l is the axial length of the infusion slit.

DISCUSSION

A novel local drug delivery method has been modeled using computational fluid dynamics and experimental fluid mechanics. These models illustrated that infusion of drugs can be efficient for preventing thrombosis and vascular lesion development which may occur over short distances distal to the infusion site. Efficient administration of clinically therapeutic drugs can be achieved adjacent to the wall using this approach since very low infusion rates were sufficient to maintain relatively high drug concentrations. The low infusion rates required therefore reduce the total volume of drug required and decrease both the cost and potential side effects of systemic drug delivery.[15]

The infusion rates required to maintain the necessary drug levels are highly dependent on the drug diffusivity and the blood flow conditions. Higher vessel wall drug concentrations are present under identical flow conditions when the drug diffusivity decreases. Low drug diffusivity limits the radial diffusion of the drug from the wall. Therefore, growth of the concentration boundary layer with axial location is slow, and near wall concentration levels remain high. The scaling analysis, presented in the previous section, relates the important parameters governing mass transport for this approach.

The infusion device has several theoretical advantages over existing local drug delivery approaches. For example, the effectiveness of coated stents is limited by the amount of active agent which can be incorporated into polymer coatings. In addition, stents typically cover only 5%–12% of the lumenal surface area.[17] Therefore, drug delivery via stents is not uniform and normal blood flow patterns may be disrupted. Delivery balloon catheters, such as the double-balloon catheter (USCI Division, C.R. Bard), cause minimal trauma to the blood vessel, but permit only brief treatment intervals since distal ischemia may occur while the balloon is inflated. Other more recently developed delivery balloon catheters deliver drugs through holes perforated in the balloon.[7,10,11,23] The disadvantage of the perforated balloon catheters is the potential for vascular trauma from the jets of drug leaving the catheter. Another potential problem with perforated devices is the tendency for occlusion of some of the holes. The result is nonuniform drug delivery. A third type of local delivery device involves electrical stimulation of diffusion of the drug towards the adventitial side of the blood vessel from the lumen (iontophoresis). While this approach may achieve higher loading of the vessel wall with drugs initially, the treatment period is again brief since the vessel is occluded, and drug washout may be rapid.

A major limitation of this quantitative study was the assumption of an impermeable wall boundary condition, although overall drug uptake by the vessel wall should be modest relative to the amount of drug convected downstream. Nonetheless, *in vivo* there may be drug uptake into the vessel wall which may influence the concentration field. In addition, only steady flow was modeled. Complex flow wave forms could be added to the numerical and experimental models. Fortunately, mass transfer can be considered quasi-steady for the Schmidt number range of most biological molecules.[14] In addition, *in vivo* studies using predicted infusion rates show inhibition of thrombus development distal to local infusion sites.[3]

It should also be noted that anatomic geometry and effects of pulsatility, as well as the multiphasic nature of blood flow, will alter the results of the computations. Clinically, the vascular segment that needs to be treated must be just distal to the infusion site. This limitation occurs as the result of secondary flows that develop from vessel curvature, ostia, bifurcations and stenoses. These secondary flow phenomena move the slow moving fluid layers adjacent to the wall towards the core of the blood flow. Pulsatility may be further explored; however, due to the laminar nature of the flow and the very slow fluid velocities close to the wall, the mean drug concentration at the wall in a pulsatile flow case should be similar to the steady flow case. Finally, the motions of blood cells increase diffusion rates; thus, actual drug concentrations at the wall may be somewhat lower than calculated values. Despite these limitations, *in vivo* studies have clearly demonstrated the usefulness of this local delivery principle.[3,15,22]

Perhaps the most attractive application of the present method is for treatment of the distal anastomosis of synthetic vascular grafts, a site where thrombus formation and tissue ingrowth commonly lead to graft failure for dialysis access and peripheral ePTFE grafts. Placement of the infusion site immediately proximal to a distal graft anastomosis would approximate closely the straight tube

conditions used in the present theoretical and experimental study. Although clinical applications would require concurrent implantation of a minipump for drug delivery, little additional surgical installation costs or clinical complications are expected. The graft infusion device should therefore be cost effective by reducing the frequency of surgical graft revision or replacement.

There are now several published animal studies documenting the efficacy of this approach. In a porcine arteriovenous shunt model, local delivery of the potent antithrombin phe-pro-arg chloromethyl ketone (PPACK) profoundly interrupted acute platelet-dependent thrombus formation without effects on systemic hemostatic parameters.[22] Local delivery of heparin into ePTFE grafts in the rabbit vena cava[3] and dog femoral vein[4] preserved graft patency at 2 weeks without systemic effects on coagulation status, whereas all grafts occluded that were comparably infused with saline only. In baboons, local infusion of the nitric oxide donor NO-proline markedly reduced early graft platelet deposition.[9,21] Infusion of the same NO donor for 1 week into canine carotid artery grafts markedly reduced vascular smooth muscle cell proliferation at the graft anastomoses and within downstream arterial segments.[2] Local infusion of the potent mitogen fibroblast growth factor (FGF) into canine carotid artery grafts increased intimal thickening by 72 at 2 weeks,[5] while infusion of the potent cytotoxin FGF-saporin reduced intimal thickening by 40%–46% in canine carotid artery grafts and femoral arteriovenous grafts after 2 weeks.[6,16] In each instance, these reductions were accomplished with small volume infusion requirements (0.5–1.0 ml/wk), and were without evidence of systemic toxicity or side effects. Thus, the efficiency of the local drug infusion approach for limiting thrombosis and the tissue response to vascular injury has been well documented *in vivo*, despite the complexities associated with surgical graft placement into a physiologic blood flow environment.

Finally, the method described here can be generally applied in the design of both vascular grafts and catheter-type devices which were similarly developed to deliver antithrombotic drugs only into the slowest moving blood layers adjacent to the vascular wall.[15] Thus, in the future the local drug infusion approach may be employed for improving outcomes after stent placement, and following other mechanical interventional procedures (e.g., angioplasty) for arterial revascularization or repair.

ACKNOWLEDGMENTS

This work was supported in part by research Grant Nos. HL 31469, HL 48667, and HL 39437-07 from the National Institutes of Health.

REFERENCES

[1] Bird, R. B., W. E. Stewart, and E. N. Lightfoot. Transport Phenomena. New York: Wiley, 1960, pp. 42–47.
[2] Chen C., S. R. Hanson, L. K. Keefer, T. C. Hutsell, J. D. Hughes, D. N. Ku, and A. B. Lumsden. Boundary layer infusion of nitric oxide reduces smooth muscle cell proliferation in the endarterectomized canine artery. *J Surg Res.* 67:26–32, 1997.
[3] Chen, C., S. R. Hanson, and A. B. Lumsden. Boundary layer infusion of heparin prevents thrombosis and reduces neointimal hyperplasia in venous polytetrafluoroethylene grafts without systemic anticoagulation, *J. Vas. Surg.* 22: 237–247, 1995.
[4] Chen C., J. D. Hughes, S. G. Mattar, S. R. Hanson, and A. B. Lumsden. Transgraft infusion of heparin prevents early thrombosis of expanded PTFE grafts in the canine femoral vein. *Ann. Vasc. Surg.* 10:147–152, 1996.
[5] Chen C., J. Li, S. G. Mattar, G. F. Pierce, L. Aukerman, S. R. Hanson, and A. B. Lumsden. Boundary layer infusion of basic fibroblast growth factor accelerates intimal hyperplasia in endarterectomized canine artery. *J Surg. Res.* 69:300–306, 1997.
[6] Chen, C., S. G. Mattar, J. D. Hughes, G. F. Pierce, J. E. Cook, D. N. Ku, S. R. Hanson, and A. B. Lumsden. Recombinant chimeric toxin, basic fibroblast growth factor-saporin, reduces venous neointinmal hyperplasia in the arteriovenous graft. *Circulation* 94:1989–1995, 1996.
[7] Cumberland, D. C., J. Gunn, D. Tsikaderis, S. Arafa, and A. Ahsan. Initial clinical experience of local drug delivery via a porous balloon during percutaneous coronary angioplasty. *J. Am. Coll. Cardiol.* 23:186A, 1994.
[8] Cussler, E. L. Diffusion. Cambridge: Cambridge University Press, 1984.
[9] Hanson, S. R., T. C. Hutsell, L. K. Keefer, D. L. Mooradian, and D. J. Smith. Nitric oxide donors: A continuing opportunity in drug design. *Adv. Pharmacol.* 34:383–398, 1995.
[10] Hong, M. K., S. C. Wong, A. Farb, M. D. Mehlman, R. Virmani, J. J. Barry, and M. B. Leon. Feasibility and drug delivery efficiency of a new balloon angioplasty catheter capable of performing simultaneous local drug delivery. *Coronary Artery Disease* 4:1023–1027, 1993.
[11] Lambert, C. R., J. E. Leone, and S. M. Rowland. Local drug delivery catheters: functional comparison of porous and microporous designs. *Coronary Artery Disease* 4:469–475, 1993.
[12] Lincoff, A. M., E. J. Topol, and S. G. Ellis. Local drug delivery for the prevention of Restenosis—Fact, fancy, and future. *Circulation* 90:2070–2084, 1994.
[13] Lovich, M. A., and E. R. Edelman. Mechanisms of transmural heparin transport in the rat abdominal aorta after local vascular delivery. *Circ. Res.* 77:1143–1150, 1995.
[14] Ma, P., X. Li, and D. N. Ku. Heat and mass transfer in a separated flow region for high Prandtl and Schmidt numbers under pulsatile conditions. *Int. J. Heat Mass Transf.* 37:2723–2736, 1994.
[15] Markou, C. P., N. F. Chronos, L. A. Harker, and S. R. Hanson. Local endovascular drug delivery for inhibition of thrombosis. *Circulation* 94:1563, 1996.
[16] Mattar, S. G., S. R. Hanson, G. F. Pierce, C. Chen, J. D. Hughes, J. E. Cook, C. Shen, B. A. Noe, C. R. Suwyn, J. R. Scott, and A. B. Lumsden. Local infusion of fibroblast growth factor-saporin reduces intimal hyperplasia. *J. Surg. Res.* 60:339–344, 1996.
[17] Muller, D. W. M., and S. G. Ellisa. Advances in coronary

angioplasty: endo-vascular stents. *Coronary Artery Disease* 1:438–448, 1990.

[18] Nathan, A., and E. R. Edelman. Local interventions for vasculoproliferative diseases. In: Molecular Interventions and Local Drug Delivery. London: Saunders, 1995, pp. 29–52.

[19] Pinchak, A. C., and S. Ostrach. Blood flow in branching vessels. *J. Appl. Physiol.* 41:646–658, 1975.

[20] Rogers, C. Thrombotic heart disease and myocardial infarction: Local therapy. In: Molecular Interventions and Local Drug Delivery. London: Saunders, 1995, pp. 131–147.

[21] Saavedra, J. E., G. Southan, K. Davies, A. Lundell, C. Markou, S. R. Hanson, C. Adrie, W. E. Hurford, W. M. Zapol, and L. K. Keefer. Localizing antithrombotic and vasodilatory activity with a novel, ultrafast nitric oxide donor. *J. Med. Chem.* 39:4361–4365, 1996.

[22] Scott, N. A., G. L. Nunes, S. B. King, L. A. Harker, and S. R. Hanson. Local delivery of an antithrombin inhibits platelet-dependent thrombosis. *Circulation* 90:1951–1955, 1994.

[23] Wolinsky, H., and S. N. Thung. Use of a perforated balloon catheter to deliver concentrated heparin into the wall of the normal canine artery. *J. Am. Coll. Cardiol.* 15:475–481, 1990.